Obesity Facts

Research Article

Obes Facts
DOI: 10.1159/000533966

Received: March 13, 2023
Accepted: August 31, 2023
Published online: October 11, 2023

Ube2L6 Promotes M1 Macrophage Polarization in High-Fat Diet-Fed Obese Mice via ISGylation of STAT1 to Trigger STAT1 Activation

Yunqian Li[a] Xiao Dong[a] Wenqian He[b] Huibiao Quan[c] Kaining Chen[c] Chaoping Cen[c] Weiping Wei[c]

[a]Center of Gerontology and Geriatrics, Hainan General Hospital, Hainan Affiliated Hospital of Hainan Medical University, Haikou, PR China; [b]Department of Endocrinology, Hainan Medical College, Haikou, PR China; [c]Department of Endocrinology, Hainan General Hospital, Hainan Affiliated Hospital of Hainan Medical University, Haikou, PR China

Keywords
Obesity · M1 macrophage polarization · Ube2L6 · STAT1 · ISG15

Abstract
Introduction: In obesity-related type 2 diabetes mellitus (T2DM), M1 macrophages aggravate chronic inflammation and insulin resistance. ISG15-conjugation enzyme E2L6 (Ube2L6) has been demonstrated as a promoter of obesity and insulin resistance. This study investigated the function and mechanism of Ube2L6 in M1 macrophage polarization in obesity. ***Methods:*** Obesity was induced in $Ube2L6^{AKO}$ mice and age-matched $Ube2L6^{flox/flox}$ control mice by high-fat diet (HFD). Stromal vascular cells were isolated from the epididymal white adipose tissue of mice. Polarization induction was performed in mouse bone marrow-derived macrophages (BMDMs) by exposure to IFN-γ, lipopolysaccharide, or IL-4. F4/80 expression was assessed by immunohistochemistry staining. Expressions of M1/M2 macrophage markers and target molecules were determined by flow cytometry, RT-qPCR, and Western blotting, respectively. Protein interaction was validated by co-immunoprecipitation (Co-IP) assay. The release of TNF-α and IL-10 was detected by ELISA. ***Results:*** The polarization of pro-inflammatory M1 macrophages together with an increase in macrophage infiltration was observed in HFD-fed mice, which could be restrained by Ube2L6 knockdown. Additionally, Ube2L6 deficiency triggered the repolarization of BMDMs from M1 to M2 phenotypes. Mechanistically, Ube2L6 promoted the expression and activation of signal transducer and activator of transcription 1 (STAT1) through interferon-stimulated gene 15 (ISG15)-mediated ISGlylation, resulting in M1 macrophage polarization. ***Conclusion:*** Ube2L6 exerts as an activator of STAT1 via post-translational modification of STAT1 by ISG15, thereby triggering M1 macrophage polarization in HFD-fed obese mice. Overall, targeting Ube2L6 may represent an effective therapeutic strategy for ameliorating obesity-related T2DM.

Introduction

Type 2 diabetes mellitus (T2DM) is an important health issue with an increasing prevalence attributed to a rising standard of living and sedentary lifestyle [1]. T2DM has been recognized as an enormous burden on the health

Yunqian Li and Xiao Dong are the co-first authors.

karger@karger.com
www.karger.com/ofa

Correspondence to:
Weiping Wei, 410233661@qq.com

systems around the world [2]. A series of metabolic diseases and different complications can be caused by T2DM because of insulin deficiency and insulin resistance [3]. Obesity, featured by excess fat deposition in various body tissues, may cause serious health problems. Obesity has been believed to be a contributor to T2DM [4]. Growing evidence has proved that obesity is a risk factor for the occurrence and development of T2DM [5]. Therefore, uncovering the potential mechanisms of T2DM in obese patients would be conducive to the prevention and treatment of these patients.

Overnourishment-induced inflammation in fatty tissues is considered an outstanding characteristic of obesity, which facilitates the progression of insulin resistance and T2DM [6]. In mouse or human white adipose tissue (WAT), multiple pro-inflammatory cytokines, including TNF-α, IL-6, and IL-1β, are released by immune cells, leading to a defect in insulin-glucose homeostasis [7, 8]. Macrophages are the major immune cells that participate in obesity-associated inflammation and insulin resistance in adipose tissues [9, 10]. Macrophages consist of two primary subgroups: activated M1 macrophages and alternatively activated M2 macrophages, which present outstanding diverse biological functions [11]. M1 macrophages expressing F4/80, CD11b, and CD11c release pro-inflammatory cytokines including TNF-α, IL-1β, IL-6, while M2 macrophages expressing F4/80, CD11b, and CD206 produce anti-inflammatory cytokines including IL-4 and IL-10. Macrophages are the crucial players for maintaining homeostasis in the fatty tissue microenvironment. M1/M2 polarization of macrophages can be driven by microenvironmental stimuli under specific conditions [12]. In obesity, the polarization of macrophages to a pro-inflammatory, called M1 macrophages, results in insulin resistance and adipose tissue dysfunction [13]. However, macrophages are prone to polarize to the anti-inflammatory phenotype (M2 macrophages) in lean fat [7]. Therefore, inhibiting the polarization of M1 macrophages represents a strategy for alleviating the pathological remodeling of WAT, thereby delaying the development of insulin resistance and T2DM.

ISG15-conjugation enzyme E2L6 (Ube2L6/UbcH8) is a specific enzyme that catalyzes ISGylation via conjugation of interferon-stimulated gene 15 (ISG15) to target proteins [14]. The conjugation of ISG15 to the lysine residues of target proteins, called ISGylation, is dependent on Ube2L6 [15]. ISGylation has been identified to exert crucial roles in type I interferon-mediated innate immune responses, which are responsible for the prevention of host cells against RNA, DNA, and retrovirus infection [16]. Notably, abnormal ISGylation resulted in macrophage polarization toward a pro-inflammatory phenotype during the SARS-CoV-2 infection [17]. Post-translational modification by ISG15 can result in the stabilization of target proteins by competitively inhibiting their ubiquitination and degradation [18]. Previous studies have showed that Ube2L6 participates in diverse pathophysiological processes, such as tumor growth [19], pathogen infection [20], and immune response [21]. Notably, Marcelin et al. [22] reported that Ube2L6 knockdown restrained adipogenesis, which was responsible for obesity resistance in mice. Moreover, a previous study by our team found that Ube2L6 deficiency protected against high-fat diet (HFD)-induced obesity, insulin resistance, and hepatic steatosis through the regulation of Atgl protein stability [23]. So far, whether Ube2L6-mediated ISGylation is involved in M1 macrophage polarization during HFD-induced obesity remains largely unknown. Interestingly, the STRING database predicted a protein association network: Ube2L6-ISG15-signal transducer and activator of transcription 1 (STAT1). Therefore, we hypothesized that Ube2L6 modulated STAT1 signaling activation via ISGylation, thus affecting M1 macrophage polarization.

To verify the above hypothesis, the Ube2L6-knockout mice were utilized, and we found that Ube2L6 deficiency suppressed HFD-induced M1 macrophage polarization in vivo. In addition, the M1 polarization of bone marrow-derived macrophages (BMDMs) was inhibited by Ube2L6 knockout in vitro. Mechanistically, Ube2L6 promoted ISGlylation of STAT1 via conjugation of ISG15 to trigger M1 macrophage polarization. Our findings shed light on the role and mechanism of Ube2L6 in M1 macrophage polarization in obesity, suggesting Ube2L6 might be a promising target for treating obesity and insulin resistance.

Methods

Clinical Samples

WATs were collected from 20 nonobese patients with body mass index (BMI) of <25 kg/m^2 and 20 obese patients with BMI of ≥30 kg/m^2 in the abdominal subcutaneous adipose tissues during surgical biopsy in Hainan General Hospital from July 2020 to July 2021. The cut-off values of BMI for nonobesity and obesity were determined in accordance with WHO/IASO/IOTF for Asian Pacific region [24]. Informed consent was collected from all individuals. The patients were excluded if they were smoker, pregnant, or had abdominopelvic surgery, hemorrhage, trauma, malignancy, cardiovascular diseases, autoimmune or lymphoproliferative diseases, gastrointestinal disease, or nephrolithiasis. Online supplementary Table 1 (for all online suppl. material, see https://doi.org/10.1159/000533966) presents the clinical characteristics of patients. The

clinical study was performed according to the Declaration of Helsinki and approved by the Medical Ethics Committee of Hainan Provincial People's Hospital.

Animal Experiments

The Ube2L6$^{flox/flox}$ mice and AdipO-Cre mice on a C57BL/6 J albino genetic background were purchased from Beijing Vital River Laboratory Animal Technology Co., Ltd. (Beijing, China). The Ube2L6$^{flox/flox}$ mice were crossbred with AdipoQ-Cre mice to generate Ube2L6^{AKO} mice. The age-matched Ube2L6$^{flox/flox}$ littermates were served as wild-type (WT) mice. For the induction of insulin resistance and obesity, the Ube2L6^{AKO} mice or WT mice were fed with 60% HFD (D12492, Research Diets, USA) for 16 weeks. The mice feeding with regular chow diet (D12450B, Research Diets) for 16 weeks were served as nonobese controls. All animal experiments were approved by the Medical Ethics Committee of Hainan Provincial People's Hospital.

Immunohistochemistry Staining

The sections of mouse adipose tissue were boiled for 10 min in sodium citrate buffer to retrieve antigens. After blocking in 2% BSA and treatment with 0.1% Triton X100, the sections were incubated with F4/80 antibody (1:500, ab6640, Abcam) overnight at 4°C. Subsequently, the sections were probed with Alexa488-conjugated secondary antibody (1:200, ab150165, Abcam), followed by counterstaining with DAPI. Under a fluorescence microscope, the sections were examined and photographed. The percentage of F4/80-positive cells was quantified using Image J software.

Isolation of Adipose Tissue Stromal Vascular Cells and Flow Cytometry

The epididymal WATs of mice were minced and digested with collagenase D (1.5 U/mL) and dispase II (2.4 U/mL) at 37°C for 60 min. After filtration with a 100-μm filter, the suspensions were subjected to centrifugation at 600 *g* for 5 min to collect stromal vascular cell (SVCs) in the bottom. The SVC pellets were treated with red blood cell lysis buffer for 5 min, followed by incubation with Fc Block for 30 min at 4°C. The SVCs were incubated with antibodies against F4/80-PE (ab105156, Abcam), CD11b-APC (ab25482, Abcam), CD206-APC (141,707, Biolegend, USA), CD11c-PE (ab210309, Abcam) for 30 min and detected on a flow cytometer (BD Biosciences, USA).

Isolation of BMDMs and Polarization Induction

BMDMs were isolated from the femurs of Ube2L6^{AKO} or WT mice. Briefly, the bone marrow was collected from the mouse femurs and filtered using the 70 μm cell strainer. After centrifugation at 250 *g* for 5 min, the bone marrow cells were cultured in BMDM medium (DMEM F12 medium containing 5% FBS (Thermo Fisher, USA), 2 mM L-glutamine, 100 units/mL penicillin, 0.1 mg/mL streptomycin, and 25 ng/mL macrophage colony-stimulating factor [M-CSF, PeproTech, USA]) for 1 week with an addition of 25 ng/mL M-CSF on day 5. The isolated BMDMs were stimulated with 100 ng/mL IFN-γ or 10 ng/mL lipopolysaccharide (LPS) for 8 h for M1 polarization or treated with 10 ng/mL IL-4 for 72 h for M2 polarization.

Cell Culture and Treatment

RAW264.7 macrophages were obtained from the American Type Culture Collection (ATCC, USA) and maintained in RPMI 1640 medium (Thermo Fisher) containing 10% FBS at 37°C with 5% CO_2. For the induction of M1 macrophage differentiation, RAW264.7 cells were stimulated with 100 ng/mL LPS for 12 h.

For cell transfection, small interfering RNA targeting Ube2L6 (si-Ube2L6) and negative control (si-NC) were purchased from GenePharma (Shanghai, China). RAW264.7 macrophages were transfected with si-Ube2L6 or si-NC using Lipofectamine 2000 (Thermo Fisher).

Real-Time Quantitative PCR

Total RNA was isolated from macrophages, SVCs, BMDMs, or human WATs using the Total RNA Extraction Kit (Solarbio, Beijing, China) and reverse transcribed into cDNA using the One Step SuperRT-PCR Mix Kit (Solarbio). The SYBR Green Real-Time PCR Master Mix (TOYOBO, Japan) was used for quantitative RT-PCR to detect target gene expression levels. The relative gene expression normalized to β-actin was calculated using the $2^{-\Delta\Delta CT}$ method. Online supplementary Table 2 lists the primer sequences used in this study.

Western Blotting

The protein extracts were obtained using modified RIPA Lysis Buffer (Beyotime, Haimen, China). Equal amount of protein samples was loaded onto SDS-PAGE and blotted onto PVDF membranes. After blocking in skimmed milk, the membranes were probed with primary antibodies against iNOS (ab205529, 1:1,000, Abcam, UK), TNF-α (ab255275, 1:1,000, Abcam), IL-10 (ab189392, 1:1,000, Abcam), Arg-1 (1:5,000, 16001-1-AP, Proteintech, Wuhan, China), ISG15 (1:1,000, 15981-1-AP, Proteintech), STAT1 (1:2,000, 10144-2-AP, Proteintech), p-STAT1 (1:1,000, ab109461, Abcam), p-JAK (bs-4163R, 1:500, Bioss, Beijing, China), JAK (bs-1439R, 1:500, Bioss), β-actin (1:1,000, 20536-1-AP, Proteintech) at 4°C overnight, followed by incubation with secondary antibody. Signals were detected using the BeyoECL Moon (Beyotime).

Co-Immunoprecipitation

The adipose tissues or RAW264.7 macrophages were lysed in RIPA Lysis Buffer in the presence of protease inhibitors. Cell lysates were centrifuged at 16,300 *g* for 10 min at 4°C. Subsequently, the Protein G agarose beads (Thermo Fisher) were conjugated with the anti-STAT1 (10144-2-AP, Proteintech) overnight at 4°C, followed by incubation with cell lysates overnight at 4°C with rotation. After washing, the immunoprecipitated proteins were eluted and subjected to Western blotting with the indicated antibodies.

Enzyme-Linked Immunosorbent Assay

The levels of TNF-α and IL-10 in the supernatants of RAW264.7 or plasmas of patients were assessed using the Mouse TNF alpha ELISA Kit (Abcam) and Human TNF alpha ELISA Kit (Abcam), Human IL-10 ELISA Kit (Abcam), respectively, following the manufacturer's instruction.

Statistical Analysis

Statistical analysis was conducted using the SPSS v23 software. Data are presented as the mean ± standard deviation (SD). Student's *t* test for two groups and a one-way ANOVA with Tukey's post-hoc test for multiple group comparison were performed.

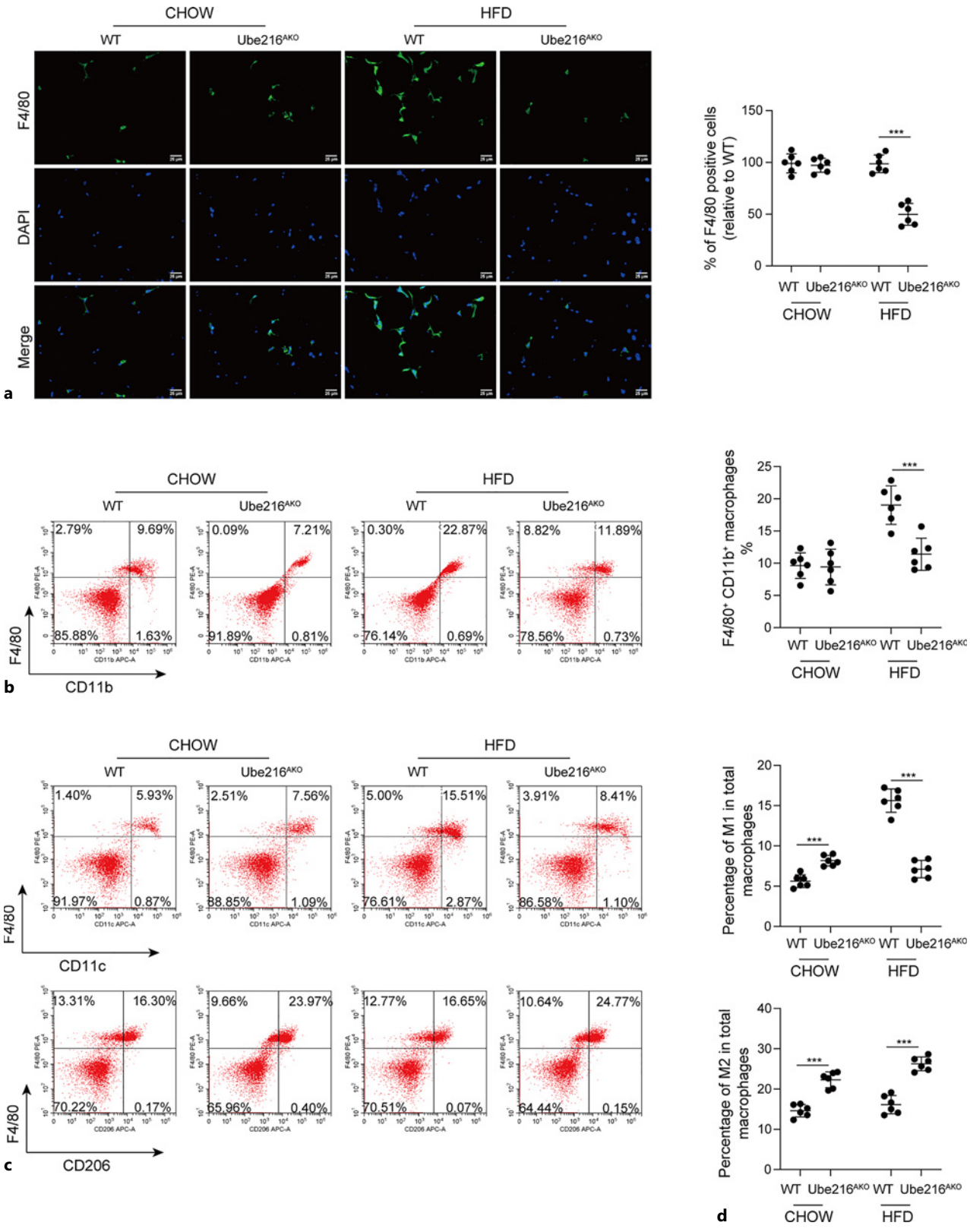

1

(For legend see next page.)

Spearman correlation analysis was used to analyze the relationship between target molecules. $p < 0.05$ was defined as statistical significance.

Results

Ube2L6 Knockout Inhibits M1 Macrophage Polarization but Promotes M2 Macrophage Polarization in HFD-Fed Obese Mice

First, the Ube2L6^{AKO} (adipose-specific knockout of Ube2L6) or WT mice were fed with HFD to induce obesity and insulin resistance. To investigate the infiltration of macrophage in adipose tissues, immunohistochemistry staining of F4/80 was carried out. Knockout of Ube2L6 remarkably reduced the percentage of F4/80 positive cells in adipose tissues of HFD-fed mice but did not affect that in regular chow diet-fed mice (Fig. 1a). In addition, we measured the percentage of SVC macrophages using flow cytometry. As shown in Figure 1b, the percentage of SVC macrophages (F4/80$^+$ and CD11b$^+$) was strikingly increased by HFD feeding as compared with regular chow, which could be reversed by Ube2L6 silencing. Furthermore, the percentage of M1 and M2 macrophages in SVC macrophages was assessed. We found that HFD-WT mice exhibited an obvious elevation in M1 macrophages (CD11c$^+$) in comparison with chow-WT mice, whereas the percentage of M2 macrophages (CD206$^+$) was not changed between HFD-WT and chow-WT mice (Fig. 1c, d). Knockout of Ube2L6 evidently lowered M1 macrophage percentage but enhanced M2 macrophage percentage in HFD-WT mice (Fig. 1c, d). These data indicate that M1 macrophage polarization is inhibited, while M2 macrophage polarization is facilitated by Ube2L6 knockout under HFD conditions.

Knockout of Ube2L6 Affects Polarized Macrophage-Mediated Inflammatory Marker Expression in HFD-Fed Obese Mice

We further explored the regulation of Ube2L6 in macrophage-mediated inflammatory marker expression. As assessed by RT-qPCR, the mRNA levels of M1 macrophage-mediated pro-inflammatory markers (TNF-α, iNOS, and IL-1β) in SVC macrophages of the HFD group were significantly elevated as compared with those in the regular chow group, which were attenuated after Ube2L6 knockout (Fig. 2a). However, Ube2L6 deficiency remarkably enhanced the mRNA levels of anti-inflammatory markers (CD206, IL-10, and Arg-1) by M2 macrophages in HFD-fed obese mice (Fig. 2b). Accordingly, the protein levels of TNF-α and iNOS were downregulated, while the protein levels of IL-10 and Arg-1 were upregulated in SVC macrophages of Ube2L6-knockout obese mice (Fig. 2c). These observations indicated that Ube2L6 knockout inhibited the expression of M1-type pro-inflammatory markers and promoted the expression of M2-type anti-inflammatory markers in HFD-fed mice.

Ube2L6 Knockout Regulates Polarization of BMDMs in Response to Different Exposures

To further validate the involvement of Ube2L6 in macrophage polarization, BMDMs were isolated from Ube2L6^{AKO} or WT mice and subjected to various exposures. After stimulation with LPS for 8 h, the expression of M1 markers (TNF-α and iNOS) was elevated in BMDMs derived from WT mice, whereas Ube2L6^{AKO} mice-derived BMDMs exhibited lower levels of TNF-α and iNOS (Fig. 3a). Similarly, treatment with IFN-γ, another inducer of M1 polarization, led to elevation in TNF-α and iNOS levels in BMDMs from WT mice. However, this alteration was weakened in IFN-γ-stimulated BMDMs from Ube2L6^{AKO} mice (Fig. 3b). On the contrary, the levels of M2 markers (CD206 and Arg-1) in IL-4F-exposed BMDMs from WT mice were lower than that from Ube2L6^{AKO} mice (Fig. 3c). Therefore, Ube2L6 deficiency contributed to M2 polarization but restrained M1 polarization of BMDMs.

STAT1 Is an ISGlylation Target of ISG15 in an Ube2L6-Dependent Manner

To gain insight into the underlying mechanism through which Ube2L6 regulated macrophage polarization in HFD-fed mice, STRING database predicated an interaction Ube2L6-ISG15-STAT1 axis (Fig. 4a). Thus, we speculated that Ube2L6 might modulate macrophage polarization through post-translational modification of STAT1 by ISG15. As validated by RT-qPCR, the mRNA levels of various interferon-stimulated genes (ISGs), including MXA, OAS1, and ISG15, were enhanced in the adipose tissues of HFD-fed mice (Fig. 4b). Besides, we observed a strong downregulation of all components of ISGylation, including ISG15, HERC5, UBE1L, and

Fig. 1. M1 macrophage polarization is inhibited but M2 macrophage polarization was promoted by Ube2L6 knockout in HFD-fed obese mice. Epididymal WAT was collected from mice. **a** IHC staining of F4/80 in WAT from different groups. **b** SVCs were isolated from epididymal WAT, and the proportion of F4/80$^+$ and CD11b$^+$ SVCs was assessed by flow cytometry. **c**, **d** Flow cytometry analysis of the proportion of CD206$^+$ and CD11c$^+$ in SVCs and quantitative analysis. Data are presented as the mean ± SD. ***$p < 0.001$ versus the indicated group.

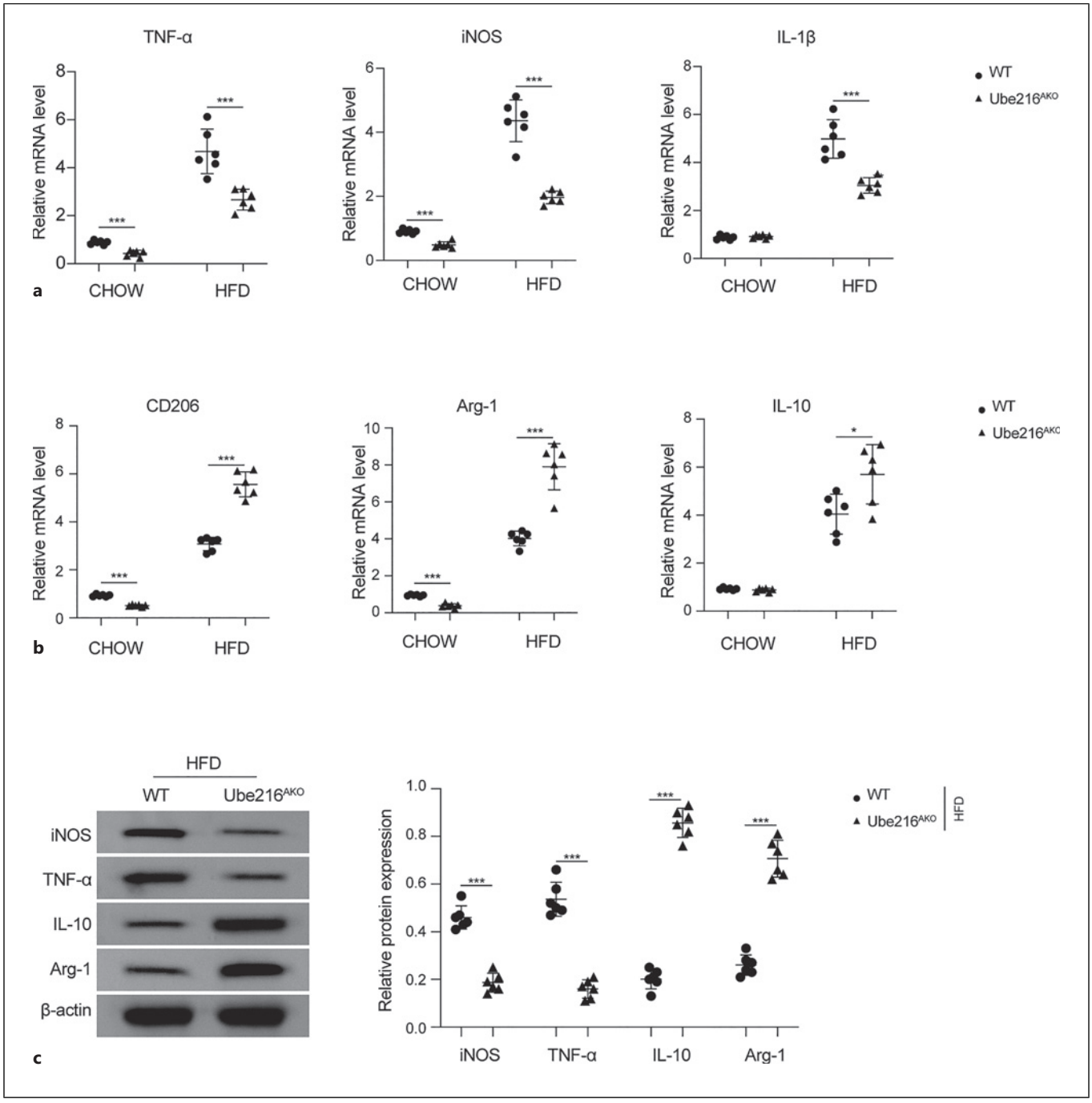

Fig. 2. Ube2L6 depletion restrains polarized macrophage-mediated inflammatory marker expression in HFD-fed obese mice. **a** Expression of M1 macrophage markers TNF-α, iNOS, and IL-1β in SVCs derived from epididymal WAT was determined by RT-qPCR. **b** RT-qPCR analysis of expression of M2 macrophage markers CD206, Arg-1, and IL-10 in SVCs. **c** Protein levels of TNF-α, iNOS, Arg-1, and IL-10 in SVCs were measured by Western blotting. Data are presented as the mean ± SD. *$p < 0.05$, ***$p < 0.001$ versus the indicated group.

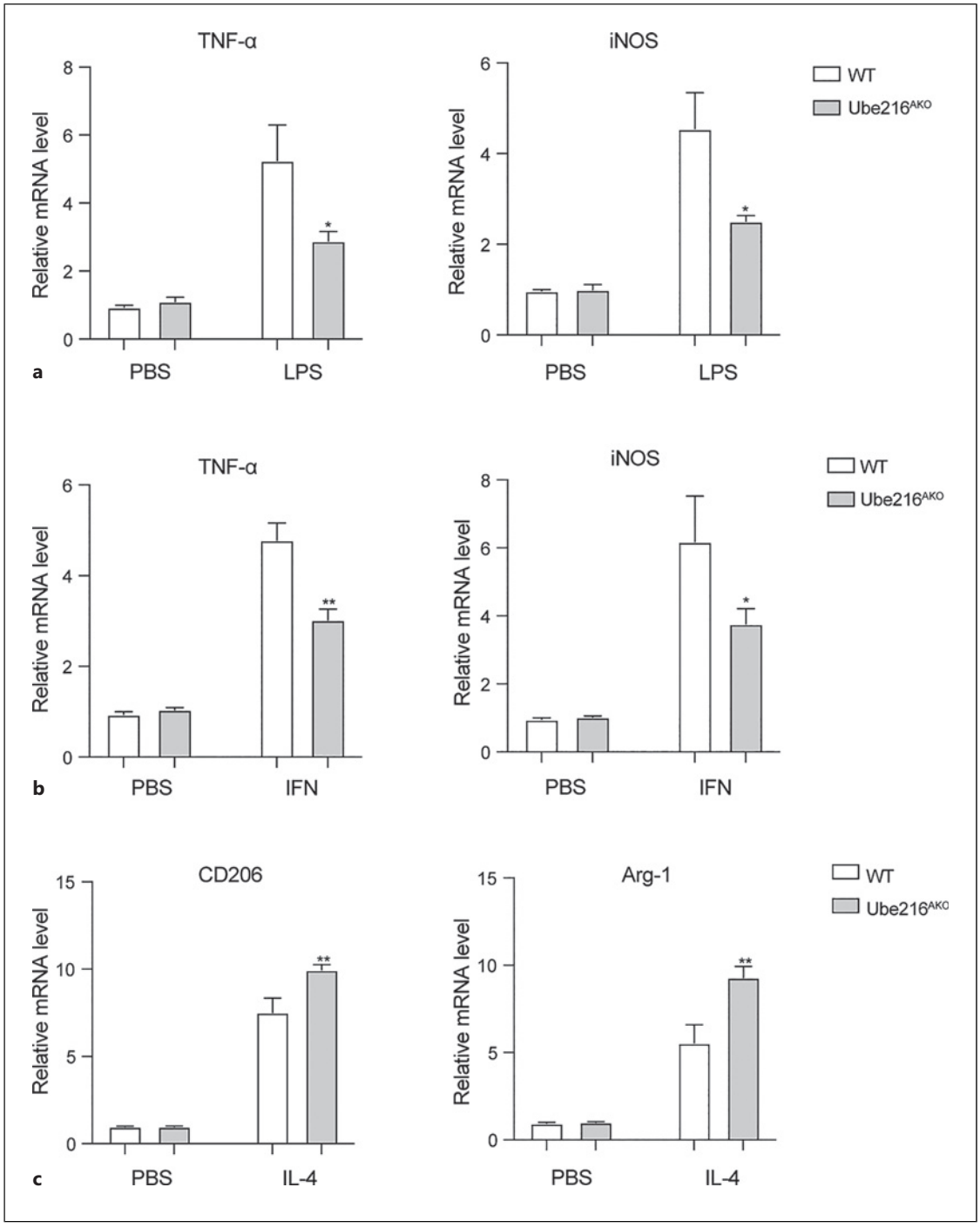

Fig. 3. Polarization of BMDMs upon different stimulations is regulated by Ube2L6. **a** BMDMs were isolated from mice and treated with 10 ng/mL LPS for 8 h. Expression of TNF-α and iNOS in BMDMs was evaluated by RT-qPCR. **b** RT-qPCR analysis of TNF-α and iNOS levels in BMDMs after treatment with 100 ng/mL IFN-γ for 8 h. **c** RT-qPCR analysis of CD206 and Arg-1 levels in BMDMs after treatment with 10 ng/mL IL-4 for 72 h. Data are presented as the mean ± SD. $*p < 0.05$, $**p < 0.01$ versus the indicated group.

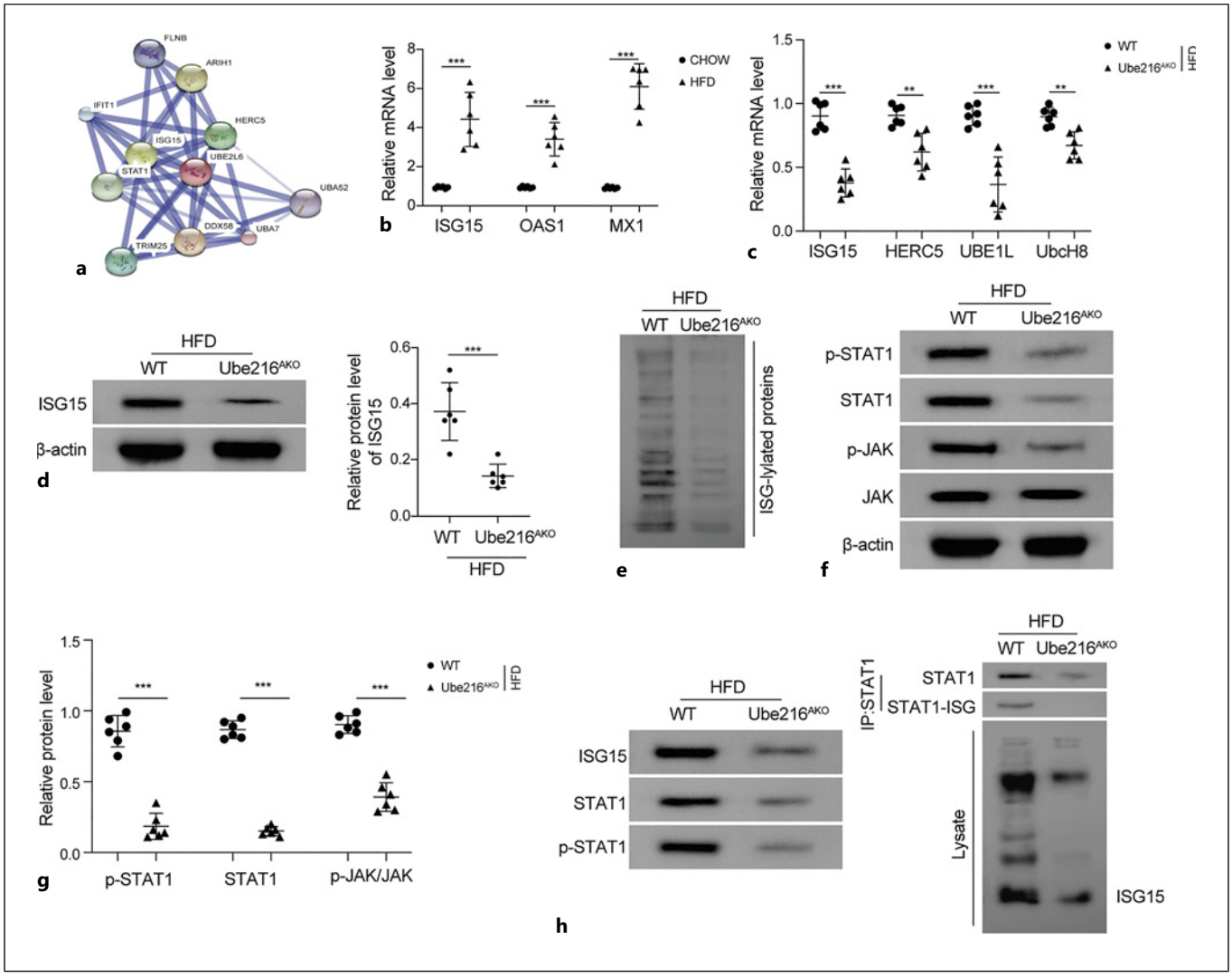

Fig. 4. Ube2L6 promotes STAT1 ISGlylation via conjugation of ISG15. **a** Interaction network of Ube2L6-ISG5-STAT1 axis was predicted by the STRING database. **b** mRNA levels of various ISGs, including MXA, OAS1, ISG15, in epididymal WAT were detected by RT-qPCR. **c** RT-qPCR analysis of levels of ISGylation components, including ISG15, HERC5, UBE1L, and UbcH8, in WAT. **d** Protein level of ISG15 in WAT was assessed by Western blotting. **e** ISG15 conjugates in protein extracts from WAT were determined by Western blotting. **f** Western blotting analysis of protein levels of p-STAT1, STAT1, p-JAK, JAK levels in WAT. **g** After immunoprecipitation by STAT1 antibody, the ISG15, STAT1, and p-STAT1 levels in WAT were measured by Western blotting. **h** Post-translational modification of STAT1 by ISG15 in WAT was evaluated by co-IP assay. Data are presented as the mean ± SD. $^{**}p < 0.01$, $^{***}p < 0.001$ versus the indicated group.

Ube2L6, in Ube2L6-knockout mice in response to HFD (Fig. 4c). Accordingly, the protein level of ISG15 was reduced in adipose tissues of HFD-fed Ube2L6^{AKO} mice (Fig. 4d). Furthermore, Ube2L6 depletion restrained the conjugation of ISG15 with protein extracts from the adipose tissues (Fig. 4e). Notably, Western blotting data indicated that the protein levels of p-STAT1, STAT1, and p-JAK were declined in the adipose tissues of Ube2L6^{AKO} mice (Fig. 4f). To verify whether STAT1 was a target of Ube2L6-mediated ISGylation, the protein extracts from macrophages were immunoprecipitated with an anti-STAT1 antibody. We found that the interaction of ISG15 with total and p-STAT1 was dramatically weakened in Ube2L6-knockout mice (Fig. 4h). Moreover, Ube2L6 knockout suppressed the conjugation of ISG15 with STAT1 protein in HFD-induced obese mice (Fig. 4h). Taken together, Ube2L6 silencing repressed the ISGlylation of STAT1 via the conjugation of ISG15 in HFD-induced obese mice.

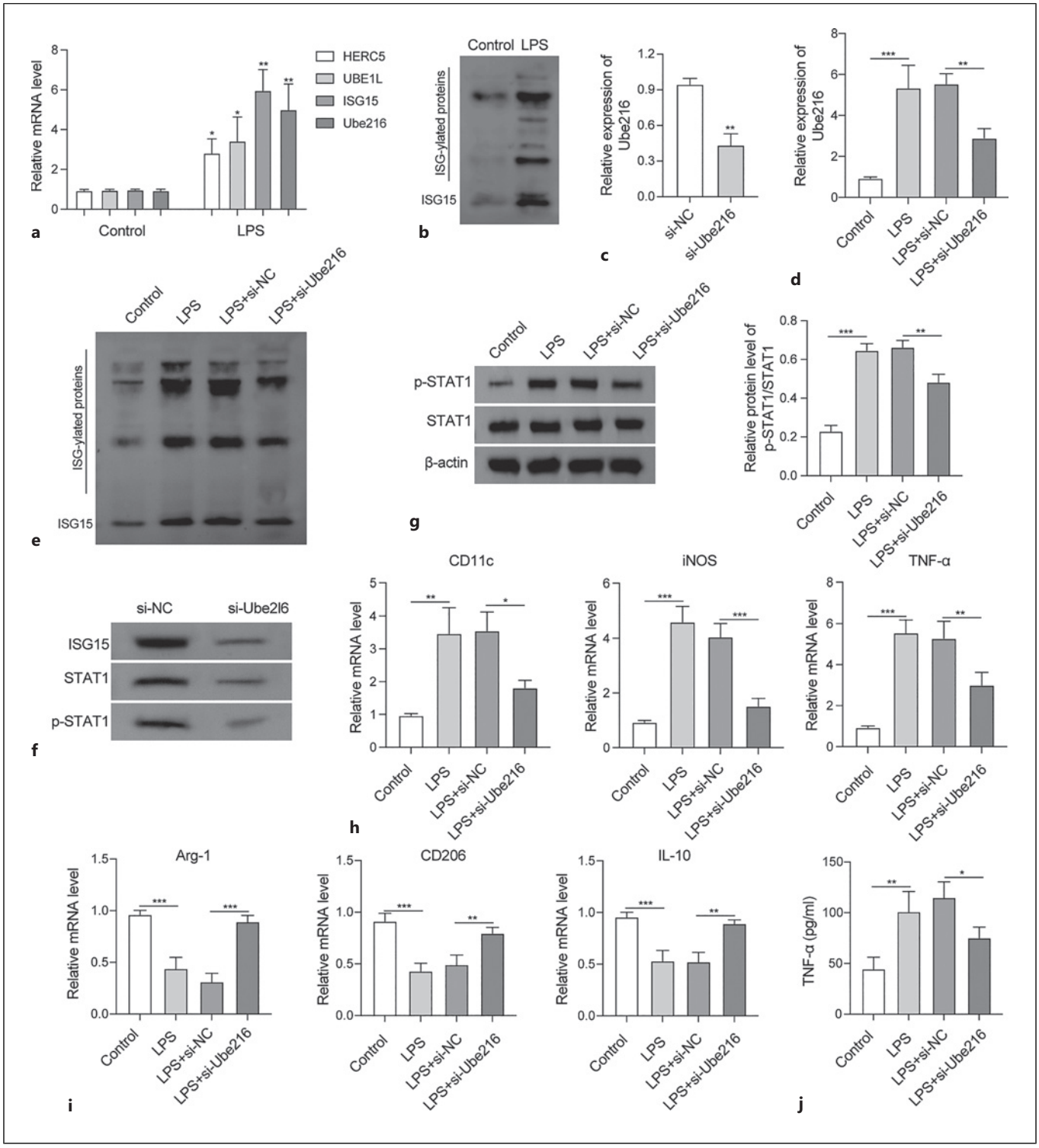

5

(For legend see next page.)

Effects and Mechanisms of Ube2L6 on LPS-Triggered M1 Macrophage Polarization in vitro

To validate the above findings in vitro, RAW264.7 macrophages were challenged with LPS for 6 h. After exposure to LPS, the expression of ISGylation components (ISG15, Ube1L, Ube2L6, and HERC5) was remarkably raised in RAW264.7 macrophages (Fig. 5a). Moreover, LPS stimulation caused upregulation of the ISG15 level together with enhancement in ISG15-conjugated proteins isolated from RAW264.7 cells (Fig. 5b). To examine the biological function of Ube2L6, RAW264.7 macrophages were transfected with si-Ube2L6 or si-NC. The silencing efficiency of Ube2L6 was validated by RT-qPCR (Fig. 5c). As expected, LPS-induced upregulation of Ube2L6 in RAW264.7 macrophages was reversed by si-Ube2L6 transfection (Fig. 5d). In addition, the reduced level of proteins conjugated with ISG15 was observed in Ube2L6-silenced RAW264.7 cells after LPS exposure (Fig. 5e). In line with the in vivo observations, the interaction of ISG15 with total and p-STAT1 after immunoprecipitation with an anti-STAT1 antibody was dramatically abolished in Ube2L6-depleted RAW264.7 cells (Fig. 5f). Besides, depletion of Ube2L6 reduced the levels of p-STAT1, as well as total STAT1 in LPS-stimulated RAW264.7 cells (Fig. 5g). Furthermore, LPS exposure resulted in upregulation of M1 macrophage markers CD11c, iNOS, and TNF-α, while downregulation of M2 macrophage markers Arg-1, CD206, and IL-10 in RAW264.7 cells, which could be counteracted by Ube2L6 knockdown (Fig. 5h, i). Similarly, the enhanced release of TNF-α after LPS stimulation was abolished in Ube2L6-depleted RAW264.7 cells (Fig. 5j). Overall, these results demonstrated that Ube2L6 knockdown restrained LPS-triggered M1 macrophage polarization via inhibiting ISG15-mediated ISGlylation of STAT1 and subsequent inactivation of STAT1.

Expression Patterns and Correlation Analysis among Ube2L6 and Macrophage-Polarized Markers in Clinical Samples

To determine the clinical relevance of Ube2L6, the differential expression of Ube2L6 and macrophage-polarized markers (iNOS, TNF-α, IL-10, Arg-1, and CD206) in WAT collected from the abdominal subcutaneous adipose tissues of obese patients and nonobese patients was investigated. Clinical characteristics of all patients are shown in online supplementary Table 1. The BMI, TC, TG, LDL-C levels were higher, while the HDL-C level was lower in the obese patients as compared with the nonobese patients (online suppl. Table 1). Moreover, as compared with nonobese patients, the protein and mRNA expression levels of Ube2L6, iNOS, TNF-α, and IL-10 were increased, while the levels of Arg-1 and CD206 were decreased in WAT of obese patients as compared with those in nonobese patients (Fig. 6a, b). Furthermore, Spearman correlation analysis showed that Ube2L6 expression level was positively correlated with M1 macrophage markers, iNOS, and TNF-α (Fig. 6c), but negatively correlated with M2 macrophage markers, Arg-1, CD206, and IL-10 in WAT of obese patients (Fig. 6d). Besides, the patients with obesity exhibited higher plasma levels of TNF-α but lower level of IL-10 in comparison with nonobese patients (Fig. 6e). These data showed the close association of Ube2L6 with macrophage-polarized markers in clinical samples of obese patients.

Discussion

T2DM is an endocrine metabolism disorder featured by insulin resistance and chronic inflammation. Macrophage-mediated inflammatory response is involved in the pathological development of insulin resistance and T2DM [25]. In obesity-associated T2DM, the infiltration of macrophages in the liver and adipose tissue contributes to chronic inflammation and impaired insulin function [26]. This study uncovered the mechanism through which macrophages are polarized and infiltrated into the adipose tissue, causing insulin resistance during T2DM. We found that Ube2L6-mediated ISGylation of STAT1 led to STAT1 activation that promoted M1 polarization of macrophages in HFD-induced mouse model of obesity and insulin resistance in vivo and LPS-stimulated RAW264.7 cells in vitro. Our

Fig. 5. Ube2L6 facilitates LPS-triggered M1 macrophage polarization through post-translational modification of STAT1 by ISG15. **a** mRNA levels of HERC5, UBE1L, ISG15, and Ube2L6 in LPS-exposed RAW264.7 cells were detected by RT-qPCR. **b** ISG15 conjugates in protein extracts from LPS-exposed RAW264.7 cells were assessed by Western blotting. **c** Silencing efficiency of Ube2L6 was validated by RT-qPCR. **d** Expression of Ube2L6 in RAW264.7 cells from different groups was detected by RT-qPCR. **e** Western blotting analysis of ISG15 conjugates in RAW264.7 cells with various treatments. **f** After immunoprecipitation by STAT1 antibody, the ISG15, STAT1, and p-STAT1 levels in RAW264.7 cells were determined by Western blotting. **g** Protein abundance of STAT1 and p-STAT1 in RAW264.7 cells was detected by Western blotting. **h**, **i** RT-qPCR analysis of TNF-α, iNOS, IL-1β, CD206, Arg-1, and IL-10 levels in RAW264.7 cells. **j** ELISA assay for detecting the content of TNF-α in the supernatants of RAW264.7 cells. Data are presented as the mean ± SD. $^{*}p < 0.05$, $^{**}p < 0.01$, $^{***}p < 0.001$ versus the indicated group.

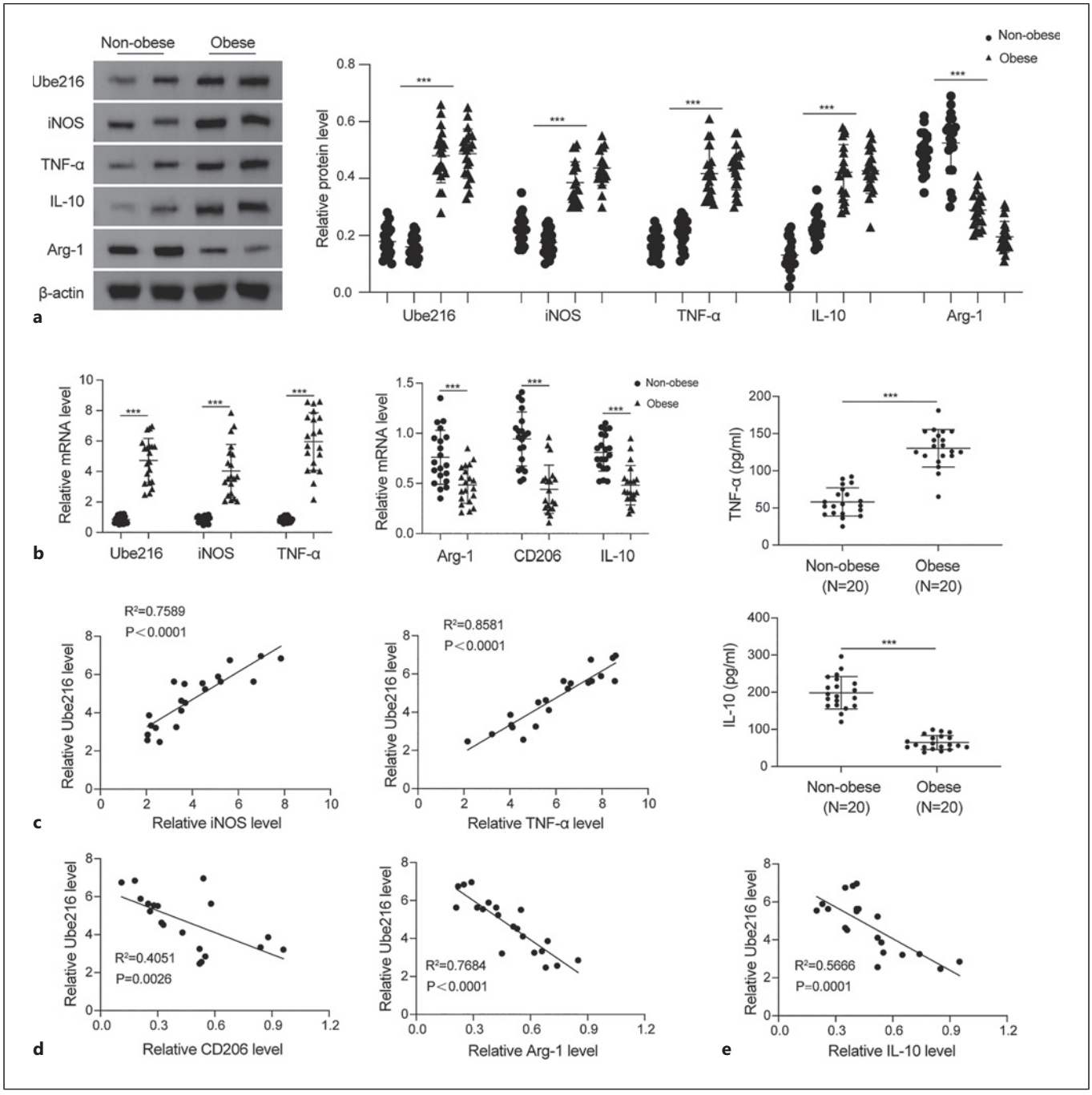

Fig. 6. Expression patterns and correlation analysis among Ube2L6 and macrophage-polarized markers in obese or nonobese patients. WATs were collected from abdominal subcutaneous adipose tissues of 20 nonobese patients (female/male: 12/8) and 20 obese patients (female/male: 9/11). **a**, **b** Expression levels of Ube2L6, TNF-α, iNOS, Arg-1, CD206, and IL-10 in WAT of obese or nonobese patients were evaluated by Western blotting and RT-qPCR. **c**, **d** Correlation analyses of Ube2L6 expression with iNOS, TNF-α, Arg-1, CD206, and IL-10 in WAT of obese patients. **e** Plasma levels of TNF-α and IL-10 in obese or nonobese patients were measured by ELISA. Data are presented as the mean ± SD. ****$p < 0.001$ versus the indicated group.

findings provide theoretical basis for the identification of novel strategy for treating inflammation and insulin resistance in obesity-associated T2DM.

During the progression of obesity, the conversion of M2 anti-inflammatory macrophages to M1 pro-inflammatory macrophages results in low-grade inflammation in adipose tissues [27]. Under this inflammatory condition, insulin resistance and T2DM may occur and progress [28]. Interestingly, Ube2L6 knockdown was reported to repress adipogenesis of 3T3-L1 adipocytes [22]. Our previous study also confirmed that knockdown of adipocyte Ube2L6 mitigated HFD-induced obesity and insulin resistance in mice [23]. This study provided the first evidence that Ube2L6 downregulation facilitated the conversion of M1 to M2 types of macrophages in the adipose tissues of HFD-fed mice. Additionally, the expression of pro-inflammatory cytokines, TNF-α, IL-1β, iNOS, was reduced by Ube2L6 knockdown. Conversely, the expression of anti-inflammatory cytokine IL-10 was enhanced by Ube2L6 deficiency. Therefore, inhibition of M1 polarization of macrophages was responsible for the inhibitory effect of Ube2L6 knockdown on insulin resistance and obesity in HFD-fed mice.

Ube2L6 has been recognized as an E2 ubiquitin and ISG15-conjugating enzyme, which exerts a vital role in regulating its target gene expression. For example, Ube2L6 promoted the transcription of ABCB6 to confer cisplatin resistance in cancer chemotherapy [29]. In this study, we found an increased expression of ISG15 after HFD feeding and LPS exposure, whereas knockdown of Ube2L6 evidently suppressed the upregulation of ISG15. Therefore, post-translational modification by ISG15 was thought to take part in the potential mechanism of Ube2L6 in macrophage polarization. JAK/STAT is the primary pathway in inflammation during which STAT1 can be phosphorylated in IFN-γ-stimulated macrophages [30]. It has been confirmed that high expression of STAT1 in activated macrophages contributes to M1 polarization and triggers the inflammatory response [31]. Here, we revealed that Ube2L6 promoted ISGylation of STAT1 via conjugation of ISG15 and then caused activation of the JAK/STAT1 pathway, thus leading to M1 polarization of macrophages in mice. More importantly, Ube2L6 was highly expressed in WAT of obese patients, which was positively associated with M1 macrophage markers but negatively associated with M2 macrophage markers. Therefore, our data provided clinical relevance of Ube2L6 to macrophage polarization in obesity. However, whether Ube2L6 can influence M1 polarization of macrophages in obese patients remains unclear and needs to be further examined. Even so, our study improves the understanding of the therapeutic potential of Ube2L6 in the treatment of inflammation and insulin resistance in obesity.

Conclusions

Taken together, Ube2L6 deletion repressed HFD-induced M1 macrophage polarization in mice. Mechanistically, Ube2L6 promoted post-translational modification of STAT1 by ISG15 to trigger the activation of the JAK/STAT1 pathway. However, other ISGylation target proteins modulated by Ube2L6 in adipocytes remain unidentified and deserve further investigation. Despite this, our findings provide novel evidence for Ube2L6 as a target for treatment of obesity-associated T2DM through repressing adipose tissue inflammation.

Acknowledgments

We would like to give our sincere gratitude to the reviewers for their constructive comments.

Statement of Ethics

This study protocol was reviewed and approved by the Medical Ethics Committee of Hainan Provincial People's Hospital, approval number 2021 272. The patient's written informed consent was obtained.

Conflict of Interest Statement

The authors declare that they have no conflict of interest.

Funding Sources

This work was supported by the Hainan Natural Science Foundation high-level Talents Project (822RC815) and project supported by the Hainan Province Clinical Medical Center.

Author Contributions

Conception and design of the study and revising the manuscript critically for important intellectual content: Weiping Wei. Acquisition of data: Huibiao Quan; Kaining Chen; and Chaoping Cen. Analysis and interpretation of data: Yunqian Li; Xiao Dong; and Wenqian He. Drafting the manuscript: Yunqian Li and Xiao Dong.

Data Availability Statement

The data underlying this article are not publicly available due to ethical reasons, which can be shared on reasonable request to the corresponding author.

References

1 Zheng Y, Ley SH, Hu FB. Global aetiology and epidemiology of type 2 diabetes mellitus and its complications. Nat Rev Endocrinol. 2018;14(2):88–98.
2 Tan C, Li B, Xiao L, Zhang Y, Su Y, Ding N. A prediction model of the incidence of type 2 diabetes in individuals with abdominal obesity: insights from the general population. Diabetes Metab Syndr Obes. 2022;15:3555–64.
3 Kautzky-Willer A, Harreiter J, Pacini G. Sex and gender differences in risk, pathophysiology and complications of type 2 diabetes mellitus. Endocr Rev. 2016;37(3):278–316.
4 Malone JI, Hansen BC. Does obesity cause type 2 diabetes mellitus (T2DM)? Or is it the opposite? Pediatr Diabetes. 2019;20(1):5–9.
5 Okamura T, Hashimoto Y, Hamaguchi M, Obora A, Kojima T, Fukui M. Ectopic fat obesity presents the greatest risk for incident type 2 diabetes: a population-based longitudinal study. Int J Obes. 2019;43(1):139–48.
6 Hotamisligil GS. Inflammation, metaflammation and immunometabolic disorders. Nature. 2017;542(7640):177–85.
7 McNelis JC, Olefsky JM. Macrophages, immunity, and metabolic disease. Immunity. 2014;41(1):36–48.
8 Greenberg AS, Reeves AR. The good and bad of adipose tissue macrophage exosomes in obesity. Cell Metab. 2021;33(4):700–2.
9 Johnson AM, Olefsky JM. The origins and drivers of insulin resistance. Cell. 2013;152(4):673–84.
10 Weisberg SP, McCann D, Desai M, Rosenbaum M, Leibel RL, Ferrante AW Jr. Obesity is associated with macrophage accumulation in adipose tissue. J Clin Invest. 2003;112(12):1796–808.
11 Hill AA, Reid Bolus W, Hasty AH. A decade of progress in adipose tissue macrophage biology. Immunol Rev. 2014;262(1):134–52.
12 Yao J, Wu D, Qiu Y. Adipose tissue macrophage in obesity-associated metabolic diseases. Front Immunol. 2022;13:977485.
13 Chawla A, Nguyen KD, Goh YP. Macrophage-mediated inflammation in metabolic disease. Nat Rev Immunol. 2011;11(11):738–49.
14 Zhao C, Beaudenon SL, Kelley ML, Waddell MB, Yuan W, Schulman BA, et al. The UbcH8 ubiquitin E2 enzyme is also the E2 enzyme for ISG15, an IFN-alpha/beta-induced ubiquitin-like protein. Proc Natl Acad Sci USA. 2004;101(20):7578–82.
15 Orfali N, Shan-Krauer D, O'Donovan TR, Mongan NP, Gudas LJ, Cahill MR, et al. Inhibition of UBE2L6 attenuates ISGylation and impedes ATRA-induced differentiation of leukemic cells. Mol Oncol. 2020;14(6):1297–309.
16 Zhang M, Li J, Yan H, Huang J, Wang F, Liu T, et al. ISGylation in innate antiviral immunity and pathogen defense responses: a review. Front Cell Dev Biol. 2021;9:788410.
17 Munnur D, Teo Q, Eggermont D, Lee HHY, Thery F, Ho J, et al. Altered ISGylation drives aberrant macrophage-dependent immune responses during SARS-CoV-2 infection. Nat Immunol. 2021;22(11):1416–27.
18 Shi HX, Yang K, Liu X, Liu XY, Wei B, Shan YF, et al. Positive regulation of interferon regulatory factor 3 activation by Herc5 via ISG15 modification. Mol Cell Biol. 2010;30(10):2424–36.
19 Zhang Q, Qiao L, Wang X, Ding C, Chen JJ. UHRF1 epigenetically down-regulates UbcH8 to inhibit apoptosis in cervical cancer cells. Cell Cycle. 2018;17(3):300–8.
20 Li L, Bai J, Fan H, Yan J, Li S, Jiang P. E2 ubiquitin-conjugating enzyme UBE2L6 promotes Senecavirus A proliferation by stabilizing the viral RNA polymerase. PLoS Pathog. 2020;16(10):e1008970.
21 Przanowski P, Loska S, Cysewski D, Dabrowski M, Kaminska B. ISG'ylation increases stability of numerous proteins including Stat1, which prevents premature termination of immune response in LPS-stimulated microglia. Neurochem Int. 2018;112:227–33.
22 Marcelin G, Liu SM, Schwartz GJ, Chua SC Jr. Identification of a loss-of-function mutation in Ube2l6 associated with obesity resistance. Diabetes. 2013;62(8):2784–95.
23 Wei W, Li Y, Li Y, Li D. Adipose-specific knockout of ubiquitin-conjugating enzyme E2L6 (Ube2l6) reduces diet-induced obesity, insulin resistance, and hepatic steatosis. J Pharmacol Sci. 2021;145(4):327–34.
24 Chattopadhyay M, Khemka VK, Chatterjee G, Ganguly A, Mukhopadhyay S, Chakrabarti S. Enhanced ROS production and oxidative damage in subcutaneous white adipose tissue mitochondria in obese and type 2 diabetes subjects. Mol Cell Biochem. 2015;399(1–2):95–103.
25 Olefsky JM, Glass CK. Macrophages, inflammation, and insulin resistance. Annu Rev Physiol. 2010;72:219–46.
26 Hotamisligil GS, Peraldi P, Budavari A, Ellis R, White MF, Spiegelman BM. IRS-1-mediated inhibition of insulin receptor tyrosine kinase activity in TNF-alpha- and obesity-induced insulin resistance. Science. 1996;271(5249):665–8.
27 Hildreth AD, Ma F, Wong YY, Sun R, Pellegrini M, O'Sullivan TE. Single-cell sequencing of human white adipose tissue identifies new cell states in health and obesity. Nat Immunol. 2021;22(5):639–53.
28 Boutens L, Stienstra R. Adipose tissue macrophages: going off track during obesity. Diabetologia. 2016;59(5):879–94.
29 Murakami M, Izumi H, Kurita T, Koi C, Morimoto Y, Yoshino K. UBE2L6 is involved in cisplatin resistance by regulating the transcription of ABCB6. Anticancer Agents Med Chem. 2020;20(12):1487–96.
30 Chen R, Wang J, Dai X, Wu S, Huang Q, Jiang L, et al. Augmented PFKFB3-mediated glycolysis by interferon-gamma promotes inflammatory M1 polarization through the JAK2/STAT1 pathway in local vascular inflammation in Takayasu arteritis. Arthritis Res Ther. 2022;24(1):266.
31 Wang A, Kang X, Wang J, Zhang S. IFIH1/IRF1/STAT1 promotes sepsis associated inflammatory lung injury via activating macrophage M1 polarization. Int Immunopharmacol. 2023;114:109478.